BMC Gastroenterology

RESEARCH

Open Access

The role of Triglyceride Glucose-Waist Circumference (TyG_WC) in predicting metabolic dysfunction-associated steatotic liver disease among individuals with hyperuricemia

Qian-Qian Wang[1,2,3†], Ning Zhang[1,4†], Xiang Xu[1,2,3], Si-Ang Lv[1,2,3], Zhuo-Deng Huang[1,2,3], Xi-Dai Long[2,3*] and Jun Wu[1,2,3*]

Abstract

Background/aims The incidence of metabolic dysfunction-associated steatotic liver disease (MASLD) among individuals with hyperuricemia is significantly high. The aim of this study was to identify effective biomarkers for the detection of MASLD among patients with hyperuricemia.

Method We conducted an analysis involving 3424 participants with hyperuricemia from the National Health and Nutrition Examination Survey (1999–2020). To identify potential significant variables, we employed Boruta's algorithm, SHapley Additive exPlanations (SHAP) and random forests. Multivariable logistic regression models were utilized to assess the odds ratio (OR) of developing MASLD. To evaluate the accuracy and clinical value of our prediction model, we employed receiver operating characteristic (ROC) curves and decision curve analysis (DCA) curves.

Results Among the study population of 3424 participants (mean [SD] age, 54 [20] years, 1788 [52.22%] males) with hyperuricemia, 1670 participants had MASLD. Using Boruta's algorithm, SHAP and random forests, our analysis suggested that Triglyceride Glucose-Waist Circumference (TyG_WC) was one of the most significant variables in predicting MASLD risk, with an area under the receiver operating characteristic (AUROC) of 0.865. The restricted curve spline (RCS) revealed a positive association between the odds ratio of TyG_WC and MASLD, when compared with lowest quantile of TyG_WC, the risk of MASLD for highest quantile was 137.96 times higher. The predictive strategy incorporating TyG_WC notably enhanced the clinical model, with threshold probabilities spanning from approximately 0% to 100%, resulting in a significant improvement of the net benefit.

Conclusions Our analysis found that TyG_WC was one of the most significant variables in predicting MASLD risk among individuals with hyperuricemia.

Keywords Metabolic dysfunction-associated steatotic liver disease, Hyperuricemia, Triglyceride Glucose-Waist Circumference (TyG_WC)

†Qian-Qian Wang and Ning Zhang contributed equally to this work.

*Correspondence:
Xi-Dai Long
sjtulongxd@263.net
Jun Wu
jun.wu@shsmu.edu.cn
Full list of author information is available at the end of the article

Introduction

Metabolic dysfunction-associated steatotic liver disease (MASLD), the latest term for steatotic liver disease associated with metabolic syndrome, is a prevalent condition currently estimated to affect up to one third of the global adult population worldwide [1]. MASLD is a common disease in which the liver accumulates excessive fat, without the presence of significant alcohol consumption. The increasing prevalence of MASLD is anticipated to rise in the coming decade, as a result of the globalization and the influence of western cultures. This trend is parallel to the growing incidence of obesity and type 2 diabetes mellitus (T2DM) [2]. In the recent years, important advances have been made in understanding the complex pathophysiological mechanisms of MASLD. The development of this MASLD is multifactorial, with an increasing focus on the role of metabolic disorders such as hyperuricemia [3], insulin resistance [4] and hyperlipidemia [5]. The recent shift in nomenclature from non-alcoholic fatty liver disease (NAFLD) to MASLD better reflects the nature of these complex systemic disorders and cardiometabolic implications of this common liver disease [6]. Given the current lack of effective therapies specifically targeted towards MASLD patients, the early diagnosis and management of MASLD are of the utmost urgency.

In contemporary society, the prevalence of hyperuricemia is also on a rapid rise, fueled by high-purine diets and sugary beverages. Uric acid, the final oxidation product of purine metabolism in humans, has been strongly linked to the development of metabolic syndrome [7–9], a cluster of conditions that include insulin resistance, dyslipidemia, hypertension, MASLD, gout, and cardiovascular diseases [10, 11]. Recent studies have extensively investigated the correlation between serum uric acid level and MASLD. A retrospective cohort study spanning 5 years suggested that serum uric acid was a predictor for the development of NAFLD in apparently healthy subjects [12]. A subsequent retrospective cohort study further reported that hyperuricemia was significantly associated with risk of developing NAFLD in non-obese subjects, and this relationship was significantly independent of clinical variables [13]. Based on three longitudinal analyses, a previous study also reported that hyperuricemia preceded the development of MASLD [14]. In addition, the study by Petta et al. demonstrated hyperuricemia related with the severity of liver damage in patients with NAFLD [15], as evidenced by the study that revealed the increase in serum uric acid levels was associated with the corresponding to the progression of NAFLD severity using controlled attenuation parameter (CAP) [16]. Additionally, a meta-analysis of 11 studies revealed that risk of NAFLD was nearly doubled in the highest serum uric acid group compared to the lowest group [17], in line with previous meta-analysis study by Liu, showing a dose–response relationship of serum uric acid with incidence of NAFLD in two prospective studies [18]. The Polistena project, which involving 61 biopsied NAFLD patients also showed that serum uric acid levels were significantly higher in patients with severe fibrosis compared to those with mild fibrosis [19]. Furthermore, the relationship between uric acid and NAFLD, regardless of metabolic syndrome features, has been consistently observed [20, 21]. In conclusion, there is an inextricable relationship between uric acid and MASLD.

The proposed hypothesis suggests that inflammation and oxidative stress serve as the fundamental connection in the relationship between uric acid and MASLD. Firstly, it has been established that uric acid can trigger an inflammatory response in the liver that is partly dependent on the NOD-, LRR- and pyrin domain-containing protein 3 (NLRP3) inflammasome [3]. This inflammatory response leads to the activation of immune cells, such as macrophages, which then accumulate lipids and contribute to the development of fatty liver [22]. Secondly, hyperuricemia has been associated with insulin resistance, a key factor in the development of fatty liver disease. Uric acid may interfere with insulin signaling, leading to decreased insulin sensitivity and increased hepatic lipid accumulation [3, 23, 24]. Thirdly, elevated uric acid levels have been linked to increased oxidative stress in the liver [3]. Oxidative stress can damage hepatocytes and contribute to the oxidation of lipoproteins, further contributing to the progression of fatty liver disease [25, 26]. Finally, uric acid may also disrupt the endocrine system, affecting the production and sensitivity of hormones related to lipid metabolism, thereby contributing to the development of fatty liver disease [27].

In general, individuals with high levels of uric acid are at a higher risk of developing MASLD. However, there are currently no effective early screening indicators specifically for this population. Therefore, it is essential to develop the new biomarkers or diagnostic tools to facilitate early detection and management of MASLD in individuals with high uric acid levels.

In our study, we investigated the potential biomarkers for detecting MASLD among patients with hyperuricemia and the role of Triglyceride Glucose-Waist Circumference (TyG_WC) in predicting metabolic dysfunction-associated steatotic liver disease among individuals with hyperuricemia.

Method

Study design and population

The datasets required for the analysis, spanning from the National Health and Nutrition Examination Survey (NHANES) conducted between 1999 and 2020, were

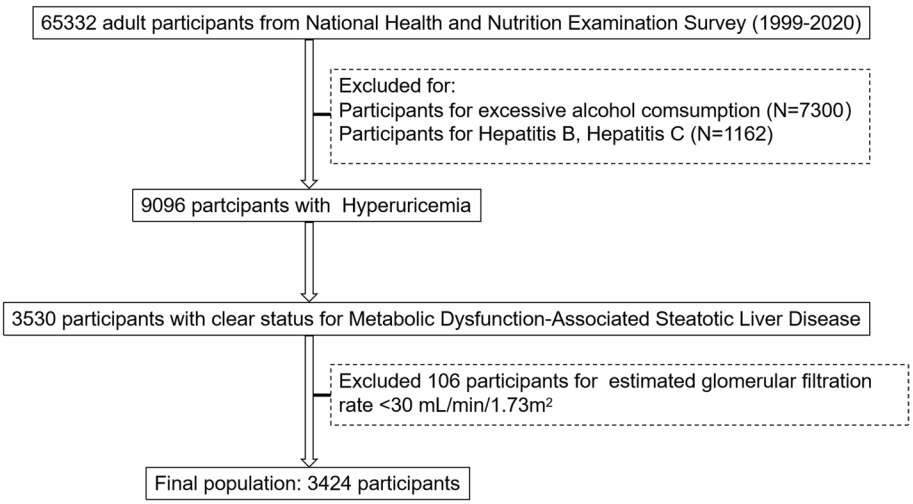

Fig. 1 Flow chart of the study population from National Health and Nutrition Examination Survey

obtained from the official NHANES website. The survey was approved by the Research Ethics Review Board at the Centers for Disease Control and Prevention (CDC) in accordance with the Declaration of Helsinki, and written informed consent was obtained from all adult participants involved in the study. All data and details of methods of assessment are available on https://www.cdc.gov/nchs/nhanes/index.htm.

In this study, we conducted an analysis involving a total of 65332 adult participants drawn from the NHANES (1999–2020). To ensure the integrity of our research, we initially excluded 7300 participants due to their significant alcohol consumption and another 1162 participants who had been diagnosed with hepatitis B/C infection. Among the remaining participants, 9096 had been diagnosed with hyperuricemia, while 3530 had a definitive status of MASLD (MASLD or non-MASLD). However, as a final step in our data preparation, we further excluded 106 individuals due to the presence of severe and end-stage renal failure, as well as dialysis patients, based on an estimated glomerular filtration rate (eGFR) of less than 30 mL/min/1.73m^2, resulting in a final study population of 3424 participants (Fig. 1).

Variables of interest

We obtained the information of socio-demographic characteristics, laboratory results, examination data, and lifestyle habits from the NHANES. The participants' age, sex, race and the ratio of family income to poverty were downloaded from demographic data. The drinking consumption, smoking status, as well as the presence of T2DM, hypertension and cardiovascular disease (CVD) were obtained from the questionnaire data. The laboratory results, including alanine aminotransferase (ALT), aspartate aminotransferase (AST), gamma-glutamyl transferase (GGT), glycohemoglobin, high-density lipoprotein (HDL), total cholesterol (TC), uric acid, fasting triglycerides, fasting blood glucose and the status of hepatitis B/C, were retrieved from the laboratory data. The ALT, AST, GGT and fasting triglycerides were measured using an enzymatic rate method with the Beckman Synchron LX20 and Beckman UniCel® DxC800 Synchron. The fasting blood glucose was measured by an enzymatic method in which glucose is converted to glucose-6-phosphate (G-6-P) by Roche C501 and Roche C311. The TC and HDL were measured using Roche Hitachi 717, Roche Hitachi 912 and Roche Modular P chemistry analyzer. The glycohemoglobin was analyzed using the hyphenated to liquid chromatography (HPLC) analytical column. The detailed description of the laboratory methods of each biochemical parameter used can be found at NHANES website.

The hepatic CAP, Body Mass Index (BMI), height and waist circumference were derived from the examination data. The Triglyceride Glucose (TyG) index was calculated as Ln (fasting triglycerides (mg/dL) × fasting blood glucose (mg/dL)/2) [28], while the Triglyceride Glucose_Body Mass Index (TyG_BMI) was calculated as TyG × BMI, TyG_WC was calculated as TyG × waist circumference and Triglyceride Glucose_Waist-to-Height Ratio (TyG_WHtR) was calculated as TyG × (waist circumference / height). The atherogenic index of plasma (AIP) was defined as log10 (triglycerides/high-density lipoprotein cholesterol) [29].

Ascertainment of MASLD and hyperuricemia

Participants from NHANES (1999–2020) were considered to have hepatic steatosis with US fatty liver

index (USFLI) score ≥ 30 [30]. We further validated our findings with another diagnostic criterion for defining hepatic steatosis using CAP values ≥ 248 dB/m [31] based on data from NHANES (2017–2020). Additionally, participants were deemed to have cardiometabolic risk factors if they met any of the following criteria:1) The BMI ≥ 25 kg/m^2 or waist circumference ≥ 94 cm for males or ≥ 80 cm for females; 2) The fasting blood glucose ≥ 100 mg/dL or a glucose level ≥ 140 mg/dL after a 2-h 75 g oral glucose tolerance test (OGTT) or haemoglobin A1c (HbA1c) level ≥ 5.7% or diagnosed as a T2DM patient or received therapy for T2DM; 3) Diagnosis of hypertension or receiving therapy for hypertension; 4) Triglyceride ≥ 150 mg/dL; 5) HDL ≤ 40 mg/dL for males or ≤ 50 mg/dL for females or receiving therapy for lowering lipids.

We finally excluded participants with iron overload or taking pharmacological agents associated with steatosis such as amiodarone, methotrexate or tamoxifen. If a participant were considered as hepatic steatosis and got one of cardiometabolic risk factors, we considered he/she was a MASLD patient.

Hyperuricemia was defined as serum uric acid level ≥ 420 μmol/L (7 mg/dL) and ≥ 360 μmol/L (6 mg/dL) in males and females, respectively [32]. The Beckman Synchron LX20 (NHANES, 1999–2007) and Beckman Coulter UniCel® DxC800 (NHANES 2008–2020) used a timed endpoint method to measure the concentration of uric acid in serum, plasma or urine. The detailed description of the laboratory methods used can be found at NHANES website.

Statistical analysis

The continuous variables were presented as the means (standard deviations [SDs]), while the categorical variables were expressed as numbers (percentages). The difference between two subgroups was compared by independent two-sample t test (continuous variables) and the chi-square test (categorical variables). The difference between the four groups according to quantiles of TyG_WC was compared by one-way analysis of variance (ANOVA) tests (continuous variables) and chi-square test (categorical variables). To select potential significant variables, we utilized Boruta's algorithm, SHapley Additive exPlanations (SHAP) and random forests. Multivariable logistic regression models were employed to assess the odds ratio (OR) and 95% confidence interval (CI) for event occurrence. The P value < 0.05 was considered to indicate statistical significance. Receiver operating characteristic (ROC) curves and decision curve analysis (DCA) curves were used to evaluate the accuracy and clinical value of prediction model. Statistical analyses were conducted using R software (version 4.4.1).

Results

Baseline characteristics

Among the 3424 individuals with hyperuricemia, 1754 participants did not have MASLD, while 1670 participants had MASLD. The basic characteristics were shown in Table 1. Compared to those without MASLD, patients with MASLD tended to be older in age, more frequently Non-Hispanic White, and married. They exhibited elevated levels of uric acid and liver enzymes such as ALT, AST, and GGT, and unfavorable metabolic profiles including lower HDL, higher AIP, TyG, BMI, TyG_BMI, TyG_WC and TyG_WHtR. Additionally, they also tended to consume less alcohol and have more cases of T2DM, cardiovascular diseases, hypertension, and thus receiving a broader range of diuretics treatments. There was no significant difference in the metabolic score for activity, the ratio of family income to poverty, smoking habits and eGFR.

Variable selection

We selected potential significant variables by using Boruta's algorithm, SHAP and random forests.

The Boruta's algorithm is a powerful technique employed to identify the most crucial features within a given dataset. It achieves this by comparing the Z-value of each feature against the Z-value of its corresponding "shadow feature." Variables with the highest feature importance scores are considered the best predictors of the dependent variable. The Boruta algorithm in our analysis suggested that TyG_WC was one of the most significant variables in predicting MASLD risk (Fig. 2).

In order to visually explain the selected variables, we used SHAP to illustrate how these variables affect the risk of MASLD. Using the SHAP approach could illustrate the importance of each selected feature in the prediction model. As shown in Fig. 3A, the bar plot displayed the mean absolute SHAP value for each feature across all predictions, serving as a measure of feature importance [33]. It displayed the top 15 most important features for the risk of MASLD. The beeswarm plot showed in Fig. 3B provided a global overview of SHAP values for selected features, with rows representing each feature ranked by the mean absolute SHAP value [33]. The bar plot and beeswarm plot both exhibited that TyG_WC served as the most important variable in predicting MASLD. In the SHAP force plot, each feature's contribution was represented by a line, with the length of the line corresponding to the SHAP value of that feature. The TyG_WC's contribution in predicting MASLD was 0.292 (Fig. 3C). At last, the SHAP dependence plot helped in understanding the sensitivity of the model to variations in a particular feature and how it contributes to the overall prediction.

Table 1 The Baseline characteristics of study population

	No MASLD (*N* = 1754)	MASLD (*N* = 1670)	*P*-Value
Age	49.74(0.60)	53.84(0.51)	< 0.001
Sex			0.50
Male	913(52.06%)	892(53.41%)	
Female	841(47.94%)	778(46.59%)	
Race			< 0.001
Mexican American	63(3.59%)	101(6.03%)	
Other Hispanic	80(4.56%)	76(4.56%)	
Non-Hispanic White	1104(62.95%)	1256(75.22%)	
Non-Hispanic Black	308(17.58%)	117(7.03%)	
Other Race	199(11.33%)	120(7.16%)	
Marital status			< 0.001
Married	980(55.87%)	1063(63.66%)	
Widowed	203(11.56%)	180(10.75%)	
Divorced	170(9.69%)	173(10.37%)	
Separated	29(1.64%)	23(1.38%)	
Never married	285(16.27%)	184(11.01%)	
Living with partner	87(4.96%)	47(2.84%)	
Uric acid	433.98(1.57)	446.59(1.81)	< 0.001
ALT (U/L)	23.21(0.37)	31.50(0.66)	< 0.001
AST (U/L)	23.93(0.34)	27.65(0.51)	< 0.001
GGT (U/L)	22.73(0.53)	37.10(1.08)	< 0.001
TC (mg/dL)	197.10(1.53)	198.24(1.42)	0.59
HDL (mg/dL)	52.45(0.51)	44.08(0.40)	< 0.001
Glycohemoglobin (%)	5.51(0.02)	5.95(0.03)	< 0.001
AIP	−0.02(0.01)	0.22(0.01)	< 0.001
TyG	8.60(0.02)	9.13(0.02)	< 0.001
TyG_WC	842.22(3.72)	1067.23(5.52)	< 0.001
TyG_BMI	246.51(1.39)	328.14(2.34)	< 0.001
TyG_WHtR	4.15(0.02)	5.56(0.04)	< 0.001
BMI (Kg/m^2)	28.64(0.15)	35.95(0.25)	< 0.001
Waist circumference (cm)	97.78(0.34)	116.84(0.54)	< 0.001
Smoking			0.44
< 100	990(56.44%)	971(58.12%)	
≥ 100	764(43.56%)	699(41.88%)	
Alcohol (g)	2.37(0.20)	1.29(0.17)	< 0.001
CVD	230(13.10%)	271(16.24%)	0.02
T2DM	237(13.50%)	717(42.92%)	< 0.001
Hypertension	855(48.74%)	1113(66.65%)	< 0.001
PA_total_MET	3521.62(266.88)	3405.18(254.31)	0.71
PIR	2.98(0.05)	3.00(0.05)	0.75
eGFR (mL/min/1.73m^2)	85.53(0.77)	83.51(0.74)	0.05
Diuretics			< 0.001
Yes	383(21.86%)	572(34.28%)	
No	669(38.12%)	404(24.21%)	
Other	702(40.03%)	693(41.51%)	

Data are expressed as numbers (weighted proportions) for categorical variables and as weighted means (Standard Deviations, SDs) for continuous variables

AIP atherogenic index of plasma, *ALT* alanine aminotransferase, *AST* aspartate aminotransferase, *BMI* body mass index (calculated as weight in kilograms divided by height in meters squared), *CVD* cardiovascular disease, *eGFR* estimated glomerular filtration rate (according to Chronic Kidney Disease Epidemiology Collaboration 2009, CKD-EPI 2009), *GGT* gamma-glutamyl transferase, *HDL* high-density lipoprotein, *PA_total_MET* metabolic score for total physical activity, *PIR* ratio of family income to poverty, *TC* total cholesterol, *TyG* Triglyceride Glucose, *TyG_BMI* TyG × BMI, *TyG_WC* TyG × waist circumference, *TyG_WHtR*, TyG × (waist circumference to height ratio), *T2DM* type 2 diabetes mellitus

As demonstrated in the Fig. 3D, the prediction ability for MASLD increased as the increase of TyG_WC.

Finally, the employment of random forest feature selection marked a crucial juncture in our data preprocessing efforts. The Gini Index, accuracy, and imitation plot were used to evaluate and select the most relevant features for the given dataset (Fig. 4). The Gini Index measures the degree of purity of each node in the tree, while the accuracy and imitation plot help in visualizing the performance of the model with different sets of features. By analyzing these metrics, the figure unambiguously revealed that TyG_WC emerged as the most significant and accurate variable. This insight not only simplified our analysis but also strengthened the model's predictive capabilities, paving the way for more reliable and effective decision-making based on our data.

Association of TyG_WC with the odds ratio of MASLD

To further investigated the association of TyG_WC with the odds ratio of MASLD, we conducted the multivariable logistic regression utilizing restricted curve spline (RCS). The RCS revealed a positive association between TyG_WC and the odds ratio of MASLD as depicted in Fig. 5. After adjusting potential important variables including age, sex, race, smoking, drinking status, hypertension, CVD and diuretics treatments when compared with lowest quantile of TyG_WC, the risk of MASLD for highest quantile was 137.96 times higher, and the positive associations were observed in both the crude model and other adjusted models (Table 2). To further validated our observations, we conducted subgroup analyses. As shown in Supplementary Table 1, the positive associations between TyG_WC and risk of MASLD were appeared in each subgroup.

The role of the TyG_WC in predicting MASLD

The ROC was a graphical representation that effectively evaluates the performance of diagnostic tests. In our analysis, the area under the receiver operating characteristic (AUROC) of TyG_WC in predicting MASLD among patients with hyperuricemia was 0.865 (Fig. 6A). This value indicated that the TyG_WC index had a high degree of accuracy in distinguishing between patients with and without MASLD with a sensitivity of 0.865. The cutoff point for the study population (NHANES, 1999–2020) was at 901.087 for TyG_WC. To further validated

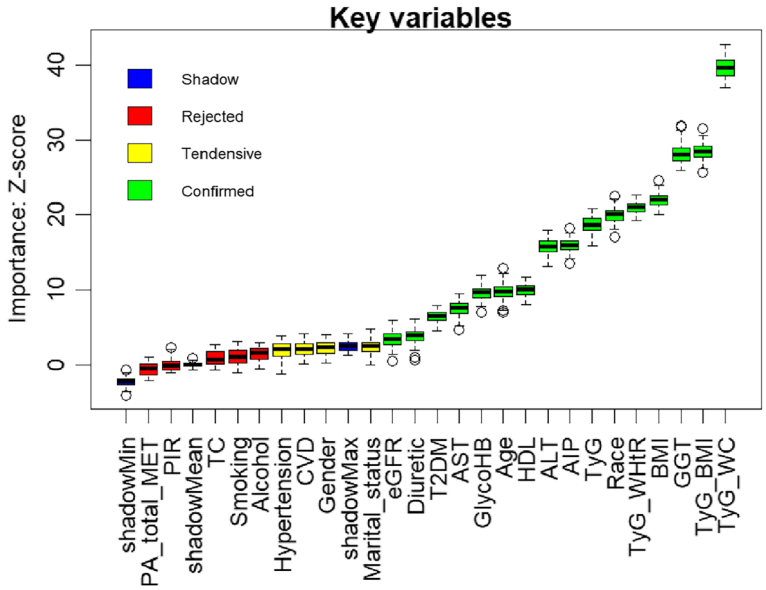

Fig. 2 Feature selection based on the Boruta's algorithm. The horizontal axis represents the name of each variable, and the vertical axis indicates the Z value of each variable. The box plot visually depicts the Z value distribution of each variable during model calculation process. The green boxes signify important variables, the yellow boxes indicate tendensive variables and red boxes signify rejected variables. AIP, atherogenic index of plasma; ALT, alanine aminotransferase; AST, aspartate aminotransferase; BMI, body mass index (calculated as weight in kilograms divided by height in meters squared); CVD, cardiovascular disease; eGFR, estimated glomerular filtration rate (according to Chronic Kidney Disease Epidemiology Collaboration 2009, CKD-EPI 2009); GGT, gamma-glutamyl transferase; GlycoHB, glycohemoglobin; HDL, high-density lipoprotein; PA_total_MET, metabolic score for total physical activity; PIR, ratio of family income to poverty; TC, total cholesterol; TyG, Triglyceride Glucose; TyG_BMI, TyG × BMI; TyG_WC, TyG × waist circumference; TyG_WHtR, TyG × (waist circumference to height ratio); T2DM, type 2 diabetes mellitus

our findings, we adopted another diagnostic criterion for defining hepatic steatosis using CAP values ≥ 248 dB/m for participants from NHANES (2017–2020). As shown in Fig. 6B, the ROC of TyG_WC in predicting MASLD was 0.814, which also signified a high level of accuracy in the prediction. Additionally, we validated the predictive performance of the TyG_WC index on the population with NAFLD with two distinct kinds of methods for the definition of NAFLD. The first definition was based on USFLI ≥ 30 (Supplementary Fig. 1), while the second definition was based on fatty liver index (FLI) ≥ 60 (Supplementary Fig. 2). As indicated in Supplementary Fig. 3, the TyG_WC index also demonstrated a robust predictive capacity in patients with NAFLD, with an AUROC of 0.868 for the first definition and an AUROC of 0.969 for the second definition.

We further plotted the DCA curve to evaluate the clinical usefulness of TyG_WC in predicting MASLD among patients with hyperuricemia. It helped to determine the clinical net benefit of using the model to make decisions about patient treatment compared to the standard of care. A well-performing DCA curve indicated that using a predictive model can lead to improved patient outcomes and resource allocation by making more informed treatment decisions based on individual patient risk. As indicated in Fig. 7, the predictive strategy incorporating TyG_WC notably enhanced the clinical model compared with other strategies that involved other potentially significant variables but did not include TyG_WC, with threshold probabilities spanning from approximately 0% to 100%, resulting in a significant improvement of the clinical net benefit.

Discussion

The NHANES database provided a large and representative sample of the US population, allowing us firstly to investigate the potential biomarkers for detecting MASLD in patients with hyperuricemia in a nationally representative manner. Based on our analysis, it was observed that TyG_WC was one of the most significant variables in predicting MASLD risk among individuals with hyperuricemia, with an AUROC of 0.865. There was a positive association between TyG_WC and the odds ratio of MASLD in both the crude model and other adjusted models. The predictive strategy incorporating TyG_WC notably enhanced the clinical model, with threshold probabilities spanning from approximately 0% to 100%, resulting in a significant improvement of the net benefit.

Currently, liver elasticity measurement is a valuable tool for assessing fatty liver disease, however its accuracy can be affected by obesity, body habitus [34] and

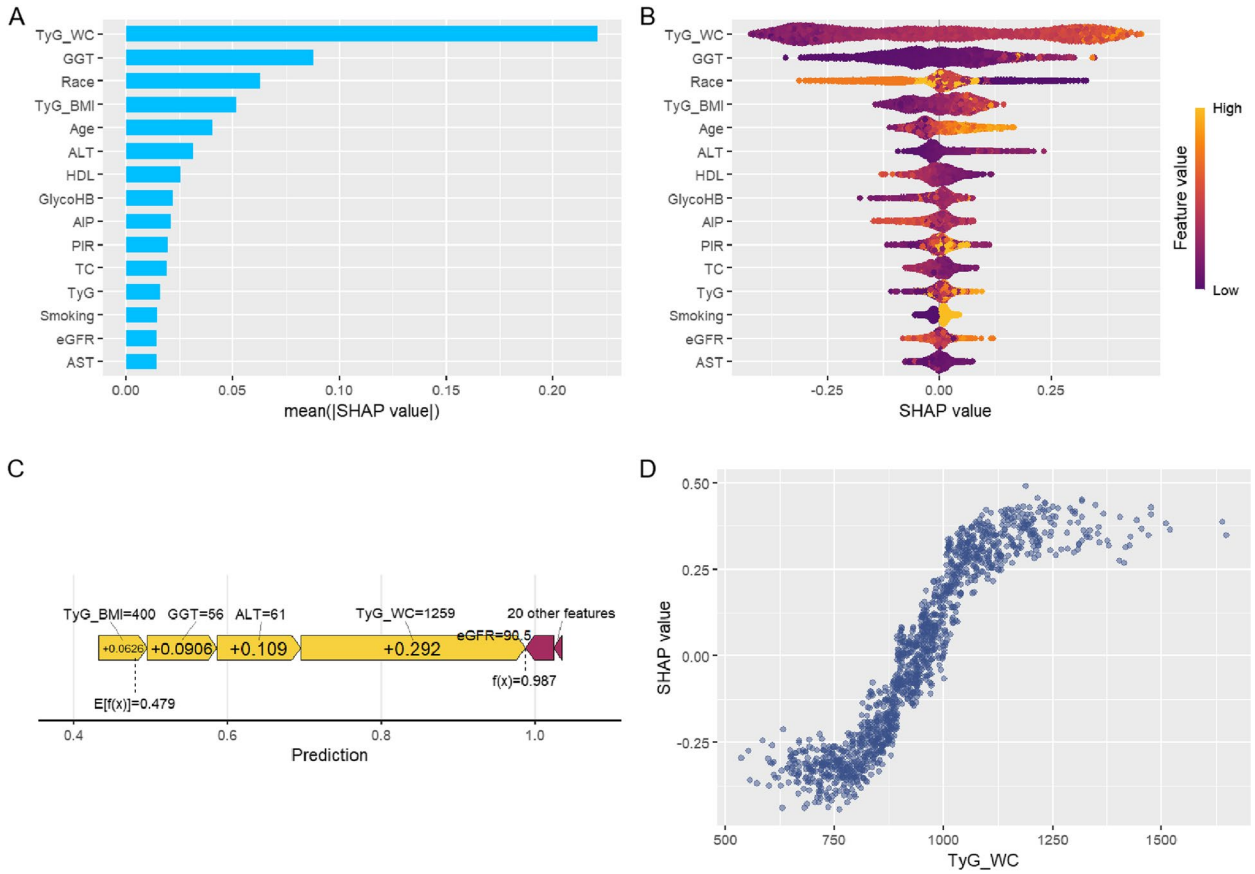

Fig. 3 Feature selection based on the SHapley Additive exPlanations (SHAP) method **A** SHAP bar plot. This bar plot displays the mean absolute SHAP value for each feature across all predictions. The height of each bar represents the average impact of a specific feature on the model's predictions. This allows for a comparative analysis of the influence of different features on the model's performance. **B** SHAP beeswarm plot. This plot provided a global overview of SHAP values for selected features, with rows representing each feature ranked by the mean absolute SHAP value. **C** SHAP force plot. Each feature's contribution was represented by a line, with the length of the line corresponding to the SHAP value of that feature. **D** SHAP dependence plot. This plot shows the relationship between a specific feature and the model's output, highlighting how changes in the feature value affect the prediction. AIP, atherogenic index of plasma; ALT, alanine aminotransferase; AST, aspartate aminotransferase; BMI, body mass index (calculated as weight in kilograms divided by height in meters squared); CVD, cardiovascular disease; eGFR, estimated glomerular filtration rate (according to Chronic Kidney Disease Epidemiology Collaboration 2009, CKD-EPI 2009); GGT, gamma-glutamyl transferase; GlycoHB, glycohemoglobin; HDL, high-density lipoprotein; PA_total_MET, metabolic score for total physical activity; PIR, ratio of family income to poverty; TC, total cholesterol; TyG, Triglyceride Glucose; TyG_BMI, TyG × BMI; TyG_WC, TyG × waist circumference; TyG_WHtR, TyG × (waist circumference to height ratio); T2DM, type 2 diabetes mellitus

operator's experience. Additionally, availability of the device may be limited in developing countries or rural areas. The development of accessible, cost-effective diagnostic biomarkers for the early and effective detection of MASLD is essential to implement preventive measures and mitigate the impact of the disease in patients with hyperuricemia. In this study, we explored the diagnostic efficacy of potential biomarkers for MASLD in American adults, finding that the TyG_WC exhibited the highest diagnostic performance by using Boruta's algorithm, SHAP model and random forest. There are several strengths by using TyG_WC as a predictor of MASLD. Firstly, by identifying hyperuricemic patients with a high risk of MASLD based on their TyG_WC score, clinicians can initiate early interventions to prevent or slow down the progression of the disease. Secondly, the TyG_WC index provides a personalized risk assessment tool that can guide tailored treatment plans for each patient, considering their unique metabolic profile. Finally, the simplicity and ease of calculating the TyG_WC index make it a cost-effective screening tool for large-scale screening programs aimed at detecting MASLD among hyperuricemic populations. In general, the TyG_WC index is a valuable tool for early detection and intervention in the management of MASLD among individuals with hyperuricemia.

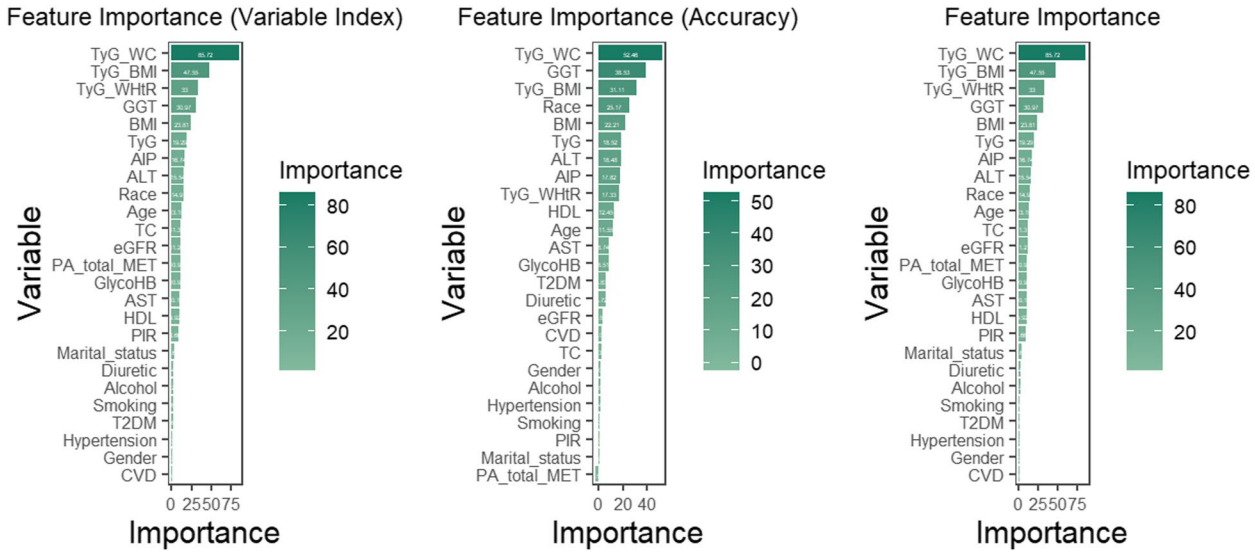

Fig. 4 Feature selection based on the random forests. The Gini Index, accuracy, and imitation plot are used to evaluate and select the most relevant features for the given dataset. The figure demonstrates how the algorithm assesses the importance of individual features by calculating their contribution to the decision trees within the forest. The Gini Index measures the degree of purity of each node in the tree, while the accuracy and imitation plot help in visualizing the performance of the model with different sets of features. By analyzing these metrics, the figure shows that certain features are more important than others in predicting the target variable, thereby providing a comprehensive understanding of the underlying data patterns. AIP, atherogenic index of plasma; ALT, alanine aminotransferase; AST, aspartate aminotransferase; BMI, body mass index (calculated as weight in kilograms divided by height in meters squared); CVD, cardiovascular disease; eGFR, estimated glomerular filtration rate (according to Chronic Kidney Disease Epidemiology Collaboration 2009, CKD-EPI 2009); GGT, gamma-glutamyl transferase; GlycoHB, glycohemoglobin; HDL, high-density lipoprotein; PA_total_MET, metabolic score for total physical activity; PIR, ratio of family income to poverty; TC, total cholesterol; TyG, Triglyceride Glucose; TyG_BMI, TyG × BMI; TyG_WC, TyG × waist circumference; TyG_WHtR, TyG × (waist circumference to height ratio); T2DM, type 2 diabetes mellitus

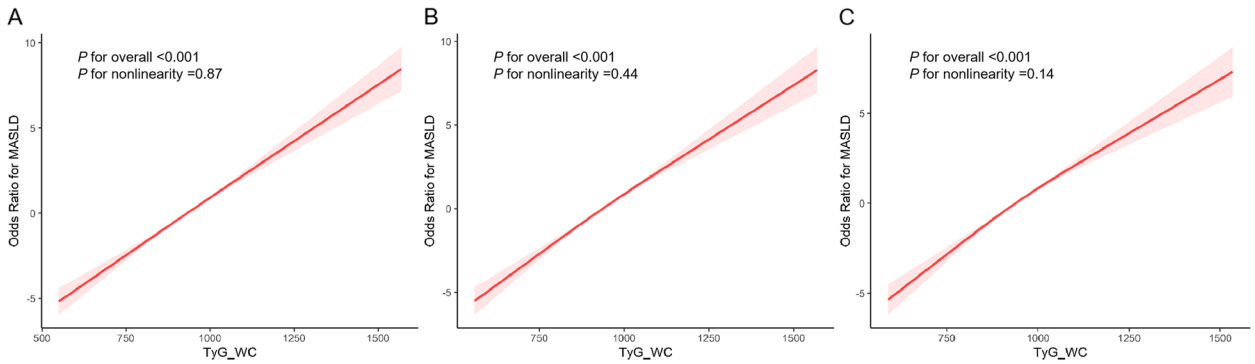

Fig. 5 Association of Triglyceride Glucose-Waist Circumference (TyG_WC) with the odds ratio of metabolic dysfunction-associated steatotic liver disease (MASLD). Multivariable Logistic regression models were employed to assess the odds ratio (OR) and 95% confidence interval (CI) for event occurrence. Odds ratio of MASLD was modeled as restricted cubic splines. **A** adjusted by age, sex and race; **B** adjusted by age, sex, race, smoking and drinking status; **C** adjusted by age, sex, race, smoking and drinking status, diuretics treatments, hypertension and cardiovascular disease

The TyG_WC index combines two components: the TyG index, a surrogate measure of insulin resistance [35, 36], and waist circumference as a proxy for abdominal obesity. High levels of insulin resistance and abdominal obesity are both known to be associated with increased risk of MASLD [37, 38]. In a Mexican cohort study, the diagnostic performance of various TyG indices in predicting MASLD was evaluated. Among these indices, the TyG_WC demonstrated good diagnostic performance, with an AUROC value of 0.84 [39]. This suggests that the TyG_WC index has a high accuracy in predicting MASLD, making it a promising tool for early detection

Table 2 Association of quantiles of TyG_WC with odds ratio of metabolic dysfunction-associated steatotic liver disease

	Crude Model		Model 1		Model 2		Model 3	
	OR (95%CI)	*P*	OR (95% CI)	*P*	OR (95%CI)	*P*	OR (95%CI)	*P*
Q1	1		1		1		1	
Q2	5.45(3.71,8.00)	< 0.001	4.87(3.30,7.20)	< 0.001	4.64(2.99,7.19)	< 0.001	5.15(3.17, 8.38)	< 0.001
Q3	19.01(13.17,27.42)	< 0.001	17.39(12.07,25.07)	< 0.001	18.29(12.37,27.04)	< 0.001	19.28(12.48, 29.77)	< 0.001
Q4	143.19(93.26,219.84)	< 0.001	138.12(89.59,212.94)	< 0.001	143.93(90.90, 227.90)	< 0.001	137.96(82.22, 231.48)	< 0.001
P for trend		< 0.001		< 0.001		< 0.001		< 0.001

OR odds ratio; Q, quantile

Crude Model: unadjusted;

Model 1: adjusted by age, sex and race;

Model 2: adjusted by age, sex, race, smoking and drinking status;

Model 3: adjusted by age, sex, race, smoking and drinking status, diuretics treatments; hypertension and cardiovascular disease

Data are expressed as numbers (weighted proportions) for categorical variables and as weighted means (Standard Deviation, SD) for continuous variables

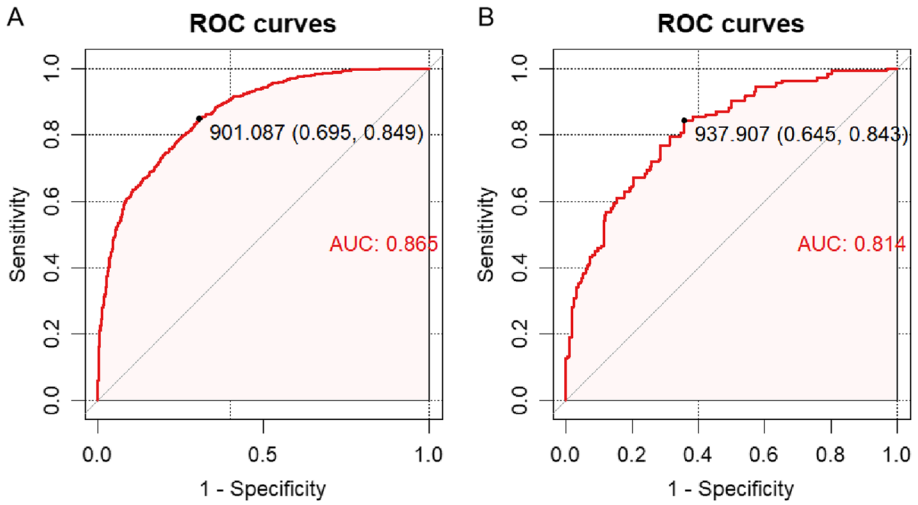

Fig. 6 The Receiver Operating Characteristic (ROC) curve. **A** The ROC curve for participants from National Health and Nutrition Examination Survey (NHANES, 1999–2020); **B** The ROC curve for participants from NHANES (2017–2020)

and management of this condition. A population-based cohort study conducted in a Japanese hospital has demonstrated a significant association between the TyG index and the incidence of NAFLD [40]. A cross-sectional study from NHANES has reported that Homeostasis Model Assessment of Insulin Resistance (HOMA-IR) and TyG_WC are core factors in predicting MASLD risk [41]. Another cross-sectional study has revealed that the TyG_WC showed considerable predictive ability with AUROC of 0.752 among Chinese T2DM patients [42]. So far, Peng H. et al. have reported the highest diagnostic performance of TyG_WC for metabolic dysfunction-associated fatty liver disease (MAFLD), achieving an AUROC of 0.90 in a population in the United States [43]. These results aligned with our findings, where the TyG_WC emerged as the most accurate predictor for MASLD among patients with hyperuricemia. Furthermore, our study proposed cutoff points for study population at 901.087 for TyG_WC. This index provides a comprehensive assessment of an individual's risk factors for MASLD, taking into account not only their body size but also other contributing factors such as insulin resistance, glucose metabolism, and other metabolic abnormalities. By using the TyG_WC index, healthcare professionals can identify patients who may be at risk of developing MASLD early on and implement appropriate interventions to prevent or manage the condition. This can lead to improved health outcomes and reduced health care costs in the long run.

In conclusion, the TyG_WC index was a promising biomarker for predicting the presence of MASLD among patients with hyperuricemia. Its integration into clinical practice can facilitate early detection, personalized treatment planning, and cost-effective management strategies

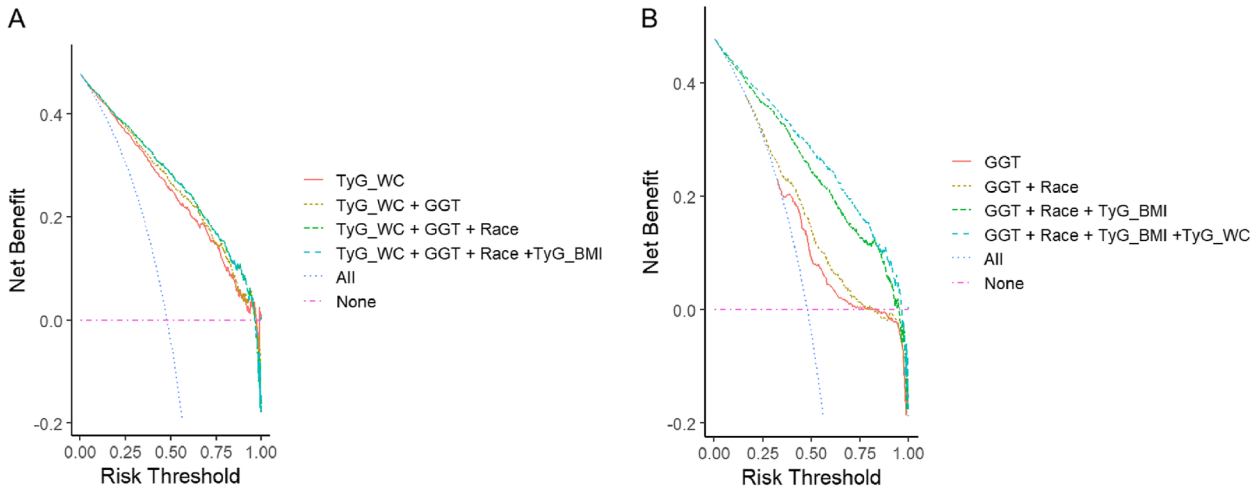

Fig. 7 The Decision Curve Analysis (DCA) curve. The x-axis of the DCA curve represents the range of possible thresholds for treating patients, typically ranging from 0% (treating all patients) to 100% (treating no patients). The y-axis represents the net benefit, which is calculated as the difference between the benefits and the harms of using the predictive model compared to the standard of care. The area under the DCA curve represents the overall performance of the model. GGT, gamma-glutamyl transferase; TyG_BMI, TyG × BMI; TyG_WC, TyG × waist circumference

for this growing health concern. Future research should focus on elucidating the underlying mechanisms and validating the TyG_WC index across diverse populations to further solidify its role as a diagnostic tool for MASLD.

Limitations and future directions

While the TyG_WC index showed promising results in predicting MASLD among patients with hyperuricemia, several limitations needed to be considered in our analysis. Cross-sectional studies cannot establish causality thus longitudinal studies are needed to confirm the temporal relationship between high TyG_WC scores and MASLD development. The TyG_WC index may not fully capture all metabolic factors contributing to MASLD. Therefore, it should be used in conjunction with other diagnostic tools and biomarkers. The generalizability of findings from studies conducted in specific populations (e.g., Asian or European populations) needs to be validated across different ethnicities and geographical regions.

Conclusions

The study highlighted the significant role of TyG_WC in predicting the risk of MASLD among individuals with hyperuricemia. Future research should focus on elucidating the pathophysiological mechanisms linking TyG_WC to MASLD in this population and exploring targeted interventions to reduce risk, particularly in hyperuricemia patients with elevated TyG_WC. Such investigations could inform evidence-based prevention and management strategies for MASLD in high-risk groups, thereby improving clinical outcomes and quality of life.

Abbreviations

AIP	Atherogenic index of plasma
ALT	Alanine aminotransferase
ANOVA	Analysis of variance
AST	Aspartate aminotransferase
AUROC	Area under the receiver operating characteristic
BMI	Body Mass Index
CAP	Controlled attenuation parameter
CDC	Centers for Disease Control and Prevention
CKD-EPI 2009	Chronic Kidney Disease Epidemiology Collaboration 2009
CI	Confidence interval
CVD	Cardiovascular disease
DCA	Decision curve analysis
eGFR	Estimated glomerular filtration rate
FLI	Fatty liver index
GGT	Gamma-glutamyl transferase
G-6-P	Glucose-6-phosphate
HbA1c	Haemoglobin A1c
HDL	High-density lipoprotein
HOMA-IR	Homeostasis Model Assessment of Insulin Resistance
HPLC	Hyphenated to liquid chromatography
MAFLD	Metabolic dysfunction-associated fatty liver disease
MASLD	Metabolic dysfunction-associated steatotic liver disease
NAFLD	Non-alcoholic fatty liver disease
NHANES	National Health and Nutrition Examination Survey
NLRP3	NOD-, LRR- and pyrin domain-containing protein 3
OR	Odds ratio
OGTT	2-Hour 75 g oral glucose tolerance test
Q	Quantile
RCS	Restricted curve spline
ROC	Receiver operating characteristic
SDs	Standard deviations
SHAP	SHapley Additive exPlanations
TC	Total cholesterol
TyG	Triglyceride Glucose
TyG_BMI	Triglyceride Glucose_Body Mass Index
TyG_WC	Triglyceride Glucose-Waist Circumference
TyG_WHtR	Triglyceride Glucose_Waist-to-Height Ratio
T2DM	Type 2 diabetes mellitus
USFLI	US fatty liver index

Supplementary Information

The online version contains supplementary material available at https://doi.org/10.1186/s12876-025-03786-2.

Supplementary Material 1.

Supplementary Material 2: Supplementary Fig. 1 Flow chart of the study population based on the US fatty liver index.

Supplementary Material 3: Supplementary Fig. 2 Flow chart of the study population based on fatty liver index.

Supplementary Material 4: Supplementary Fig. 3 The Receiver Operating Characteristic (ROC) curve for non-alcoholic fatty liver disease (NAFLD). A The ROC curve for NAFLD based on the US fatty liver index. B The ROC curve for NAFLD based on the fatty liver index.

Acknowledgements
Not applicable.

Authors' contributions
Q, W and N, Z: performed the statistical analysis, interpreted data, wrote the manuscript; X, X; S, L and Z, H: discussed the results and reviewed the final manuscript; X, L and J, W: designed the study, interpreted data and revised the manuscript; all authors read and approved the final version of the manuscript.

Funding
This work was sponsored in part by the National Natural Science Foundation of China (No. 82072892), the Key Discipline Construction project of Jiading District Health System (No. XK202405), the Natural Science Foundation of Guangxi (No.2023GXNSFAA026276), Building Projects of Guangxi Bagui Scholars (No. Guirencaiban-2024-29) and the Research Project of Jiading District Health Commission (No. 2024-KY-ZD-11 and No. 2022-QN-02).

Data availability
The data used in this study are publically available in the NHANES database (www.cdc.gov/nchs/nhanes).

Declarations

Ethics approval and consent to participate
NHANES was approved by the Research Ethics Review Board at the Centers for Disease Control and Prevention in accordance with the Declaration of Helsinki, and written informed consent was obtained from all adult participants involved in the study.

Consent for publication
Not applicable.

Competing interests
The authors declare no competing interests.

Author details
[1]Department of Laboratory Medicine, Jiading Branch of Shanghai General Hospital, Shanghai Jiao Tong University School of Medicine, Shanghai 201803, China. [2]Department of Pathology, the Affiliated Hospital of Youjiang Medical University for Nationalities, Baise 533000, China. [3]Department of Basic Research, Key Laboratory of Tumor Molecular Pathology of Guangxi Higher Education Institutes, Baise 533000, China. [4]Medical Research and Education Center, Jiading Branch of Shanghai General Hospital, Shanghai Jiao Tong University School of Medicine, Shanghai 201803, China.

Received: 8 January 2025 Accepted: 14 March 2025
Published online: 04 April 2025

References

1. Wong VW-S, Ekstedt M, Wong GL-H, Hagström H. Changing epidemiology, global trends and implications for outcomes of NAFLD. J Hepatol. 2023;79(3):842–52.
2. Qi X, Li J, Caussy C, Teng G-J, Loomba R. Epidemiology, screening, and co-management of type 2 diabetes mellitus and metabolic dysfunction–associated steatotic liver disease. Hepatology. 2024. https://doi.org/10.1097/HEP.0000000000000913. Online ahead of print.
3. Wan X, Xu C, Lin Y, Lu C, Li D, Sang J, et al. Uric acid regulates hepatic steatosis and insulin resistance through the NLRP3 inflammasome-dependent mechanism. J Hepatol. 2016;64(4):925–32.
4. Tanase DM, Gosav EM, Costea CF, Ciocoiu M, Lacatusu CM, Maranduca MA, et al. The Intricate Relationship between Type 2 Diabetes Mellitus (T2DM), Insulin Resistance (IR), and Nonalcoholic Fatty Liver Disease (NAFLD). J Diabetes Res. 2020;2020:1–16.
5. Jones AK, Bajrami B, Campbell MK, Erzurumluoglu AM, Guo Q, Chen H, et al. mARC1 in MASLD: Modulation of lipid accumulation in human hepatocytes and adipocytes. Hepatol Comm. 2024;8(5):e0365.
6. Targher G, Byrne CD, Tilg H. MASLD: a systemic metabolic disorder with cardiovascular and malignant complications. Gut. 2024;73(4):691–702.
7. Andres-Hernando A, Cicerchi C, Kuwabara M, Orlicky DJ, Sanchez-Lozada LG, Nakagawa T, et al. Umami-induced obesity and metabolic syndrome is mediated by nucleotide degradation and uric acid generation. Nat Metab. 2021;3(9):1189–201.
8. Kanbay M, Jensen T, Solak Y, Le M, Roncal-Jimenez C, Rivard C, et al. Uric acid in metabolic syndrome: From an innocent bystander to a central player. Eur J Intern Med. 2016;29:3–8.
9. Maloberti A, Tognola C, Garofani I, Algeri M, Shkodra A, Bellantonio V, et al. Uric acid and metabolic syndrome: Importance of hyperuricemia cut-off. Int J Cardiol. 2024;417:132527.
10. Li B, Chen L, Hu X, Tan T, Yang J, Bao W, et al. Association of serum uric acid with all-cause and cardiovascular mortality in diabetes. Diabetes Care. 2023;46(2):425–33.
11. Stewart DJ, Langlois V, Noone D. Hyperuricemia and Hypertension: Links and Risks . Integrated Blood Pressure Control. 2019;12:43–62.
12. Lee JW, Cho YK, Ryan† MC, Kim‡ H, Lee SW, Chang E, et al. Serum uric acid as a predictor for the development of nonalcoholic fatty liver disease in apparently healthy subjects: a 5-year retrospective cohort study. Gut and Liver. 2010;4(3):378–83.
13. Targher G, Yang C, Yang S, Xu W, Zhang J, Fu W, et al. Association between the hyperuricemia and nonalcoholic fatty liver disease risk in a Chinese population: A retrospective cohort study. Plos One. 2017;12(5):e0177249.
14. Ma Z, Zhang J, Kang X, Xu C, Sun C, Tao L, et al. Hyperuricemia precedes non-alcoholic fatty liver disease with abdominal obesity moderating this unidirectional relationship: Three longitudinal analyses. Atherosclerosis. 2020;311:44–51.
15. Petta S, Cammà C, Cabibi D, Di Marco V, Craxì A. Hyperuricemia is associated with histological liver damage in patients with non-alcoholic fatty liver disease. Aliment Pharmacol Ther. 2011;34(7):757–66.
16. Feng Y, Zheng S, Liu L, Yang Y. Association of serum uric acid with hepatic steatosis detected by controlled attenuation parameter in the United States population. Lipids in Health Dis. 2023;22(1):76.
17. Darmawan G, Hamijoyo L, Hasan I. Association between serum uric acid and non-alcoholic fatty liver disease: a meta-analysis. Acta Med Indones. 2017;49(2):136–47.
18. Liu Z, Que S, Zhou L, Zheng S. Dose-response relationship of serum uric acid with metabolic syndrome and non-alcoholic fatty liver disease incidence: a meta-analysis of prospective studies. Sci Rep. 2015;5(1):14325.
19. Bugianesi E, Manzini P, D'Antico S, Vanni E, Longo F, Leone N, et al. Relative contribution of iron burden, HFE mutations, and insulin resistance to fibrosis in nonalcoholic fatty liver. Hepatology. 2004;39(1):179–87.
20. Zheng X, Gong L, Luo R, Chen H, Peng B, Ren W, et al. Serum uric acid and non-alcoholic fatty liver disease in non-obesity Chinese adults. Lipids Health Dis. 2017;16(1):202.

21. Sirota JC, McFann K, Targher G, Johnson RJ, Chonchol M, Jalal DI. Elevated serum uric acid levels are associated with non-alcoholic fatty liver disease independently of metabolic syndrome features in the United States: Liver ultrasound data from the National Health and Nutrition Examination Survey. Metabolism. 2013;62(3):392–9.
22. Petrasek J, Iracheta-Vellve A, Saha B, Satishchandran A, Kodys K, Fitzgerald KA, et al. Metabolic danger signals, uric acid and ATP, mediate inflammatory cross-talk between hepatocytes and immune cells in alcoholic liver disease. J Leukoc Biol. 2015;98(2):249–56.
23. He F, Wang M, Zhao H, Xie D, Lv J, Liu W, et al. Autophagy protects against high uric acid-induced hepatic insulin resistance. Mol Cell Endocrinol. 2022;547:111599.
24. Zhu Y, Hu Y, Huang T, Zhang Y, Li Z, Luo C, et al. High uric acid directly inhibits insulin signalling and induces insulin resistance. Biochem Biophys Res Commun. 2014;447(4):707–14.
25. Clare K, Dillon JF, Brennan PN. Reactive oxygen species and oxidative stress in the pathogenesis of MAFLD. J Clin Transl Hepatol. 2022;10(5):939–46.
26. LeFort KR, Rungratanawanich W, Song BJ. Contributing roles of mitochondrial dysfunction and hepatocyte apoptosis in liver diseases through oxidative stress, post-translational modifications, inflammation, and intestinal barrier dysfunction. Cell Mol Life Sci. 2024;81(1):34.
27. Xie H, Li N, Zhou G, He Z, Xu X, Liu Q, et al. The association between the thyroid feedback quantile-based index and serum uric acid in U.S. adults. Eur J Med Res. 2023;28(1):259.
28. da Silva A, Caldas APS, Hermsdorff HHM, Bersch-Ferreira ÂC, Torreglosa CR, Weber B, et al. Triglyceride-glucose index is associated with symptomatic coronary artery disease in patients in secondary care. Cardiovasc Diabetol. 2019;18(1):89.
29. Shi Y, Wen M. Sex-specific differences in the effect of the atherogenic index of plasma on prediabetes and diabetes in the NHANES 2011–2018 population. Cardiovasc Diabetol. 2023;22(1):19.
30. Ruhl CE, Everhart JE. Fatty liver indices in the multiethnic United States National Health and Nutrition Examination Survey. Aliment Pharmacol Ther. 2014;41(1):65–76.
31. Karlas T, Petroff D, Sasso M, Fan J-G, Mi Y-Q, de Lédinghen V, et al. Individual patient data meta-analysis of controlled attenuation parameter (CAP) technology for assessing steatosis. J Hepatol. 2017;66(5):1022–30.
32. Johnson RJ, Bakris GL, Borghi C, Chonchol MB, Feldman D, Lanaspa MA, et al. Hyperuricemia, acute and chronic kidney disease, hypertension, and cardiovascular disease: report of a scientific workshop organized by the National Kidney Foundation. Am J Kidney Dis. 2018;71(6):851–65.
33. Ponce-Bobadilla AV, Schmitt V, Maier CS, Mensing S, Stodtmann S. Practical guide to SHAP analysis: Explaining supervised machine learning model predictions in drug development. Clin Transl Sci. 2024;17(11):e70056.
34. Petta S, Di Marco V, Cammà C, Butera G, Cabibi D, Craxì A. Reliability of liver stiffness measurement in non-alcoholic fatty liver disease: the effects of body mass index. Aliment Pharmacol Ther. 2011;33(12):1350–60.
35. Vineetha KRN, Praseeda S, Mohan TS, Sanjay K. Triglyceride Glucose (TyG) Index: A surrogate biomarker of insulin resistance. J Pakistan Med Assoc. 2022;72(5):986–8.
36. Pan J, Huang X, Wang Q, Sun J, Zhai Z, Mo J, et al. Triglyceride glucose index is strongly associated with a fragility fracture in postmenopausal elderly females with type 2 diabetes mellitus combined with osteoporosis: a 6-year follow-up study. Clin Interv Aging. 2023;18:1841–9.
37. Mucinski JM, Salvador AF, Moore MP, Fordham TM, Anderson JM, Shryack G, et al. Histological improvements following energy restriction and exercise: The role of insulin resistance in resolution of MASH. J Hepatol. 2024;81(5):781–93.
38. Shen W, Middleton MS, Cunha GM, Delgado TI, Wolfson T, Gamst A, et al. Changes in abdominal adipose tissue depots assessed by MRI correlate with hepatic histologic improvement in non-alcoholic steatohepatitis. J Hepatol. 2023;78(2):238–46.
39. Priego-Parra BA, Reyes-Diaz SA, Ordaz-Alvarez HR, Bernal-Reyes R, Icaza-Chávez ME, Martínez-Vázquez SE, et al. Diagnostic performance of sixteen biomarkers for MASLD: A study in a Mexican cohort. Clin Res Hepatol Gastroenterol. 2024;48(7):102400.
40. Kitae A, Hashimoto Y, Hamaguchi M, Obora A, Kojima T, Fukui M. The triglyceride and glucose index is a predictor of incident nonalcoholic fatty liver disease: a population-based cohort study. Can J Gastroenterol Hepatol. 2019;2019:5121574.
41. Chen H, Zhang J, Chen X, Luo L, Dong W, Wang Y, et al. Development and validation of machine learning models for MASLD: based on multiple potential screening indicators. Front Endocrinol (Lausanne). 2024;15:1449064.
42. Hu M, Yang J, Gao B, Wu Z, Wu Y, Hu D, et al. Prediction of MASLD using different screening indexes in Chinese type 2 diabetes mellitus. Diabetol Metab Syndr. 2025;17(1):10.
43. Peng H, Pan L, Ran S, Wang M, Huang S, Zhao M, et al. Prediction of MAFLD and NAFLD using different screening indexes: A cross-sectional study in U.S. adults. Front Endocrinol. 2023;14:1083032.

Publisher's Note